SvedbergOpen
DISSEMINATION OF KNOWLEDGE

International Journal of Artificial Intelligence and Machine Learning

Publisher's Home Page: https://www.svedbergopen.com/

Research Paper Open Access

# Deep Learning Assisted Microstrip Antenna System for Non-invasive Early Detection of Kidney Cancer

Naresh Rana[1], Shruti Jain[1*], Sunil Kumar Khah[2*]

[1]Department of Electronics and Communication Engineering, Jaypee University of Information Technology, Solan
[2]Department of Physics and Material Sciences, Jaypee University of Information Technology, Solan
*jain.shruti15@gmail.com, sunil.khah@juitsolan.in

**Abstract**
Kidney cancer is a serious health problem worldwide, requiring novel diagnostic tools and strategies to enable early detection, ultimately enhancing patient prognosis. This study explores a Deep Learning supported Micro Strip Antenna system for non-invasive detection of kidney cancer using Electromagnetic Sending technique and Intelligent Classifier. The first one is using deep learning models like the conventional CNNs and transfer learning-based architectures like MobileNetV2, EfficientNetB0 and SqueezeNet for classifying kidney tumors on computed tomography (CT) images. When accuracy, precision, recall, F1-score and AUC were used to evaluate the performance of all models, MobileNetV2 showed the highest classification performance having the F1-score of 97.04%. The second method involved designing and studying a microstrip patch antenna at 2.4 GHz to be used in the detection of a tumor using electromagnetic radiation. The antenna exhibited excellent impedance matching, low reflection coefficient (S11), stable VSWR characteristics, and a maximum gain of approximately 3.43 dB, ensuring efficient signal transmission and minimal power loss. The antenna had good impedance matching, low reflection coefficient (S11), and stable VSWR performance, allowing for efficient signal transmission and reducing power loss. The optimized antenna structure allows for the effective interaction with kidney tissues, for reliable non-invasive sensing of cancerous abnormalities. The integrated framework shows the potential of deep learning and microstrip technologies for accurate, cost-effective, and non-invasive early detection of kidney cancer and advanced biomedical diagnostic applications.

**Keywords:** Kidney cancer, deep learning, microstrip patch antenna, electromagnetic sensing, non-invasive diagnostics.

## 1. Introduction

Kidney cancer is the ninth most common cancer in men and 13th overall globally, contributing significantly to cancer-related morbidity and mortality, with incidence rising with age [1, 2]. Despite advancements in imaging technologies, challenges remain in distinguishing kidney tumors due to variability in imaging quality, observer interpretation, and tumor heterogeneity [3]. The most common type of kidney cancer is renal cell carcinoma (RCC), which includes several subtypes. Some of these subtypes include clear cell renal cell carcinoma, papillary renal cell carcinoma, chromophobe renal cell carcinoma, and a type of chromophobe renal cell carcinoma known for membranous c-kit positivity. visual representation of these types is shown in Figure 1.

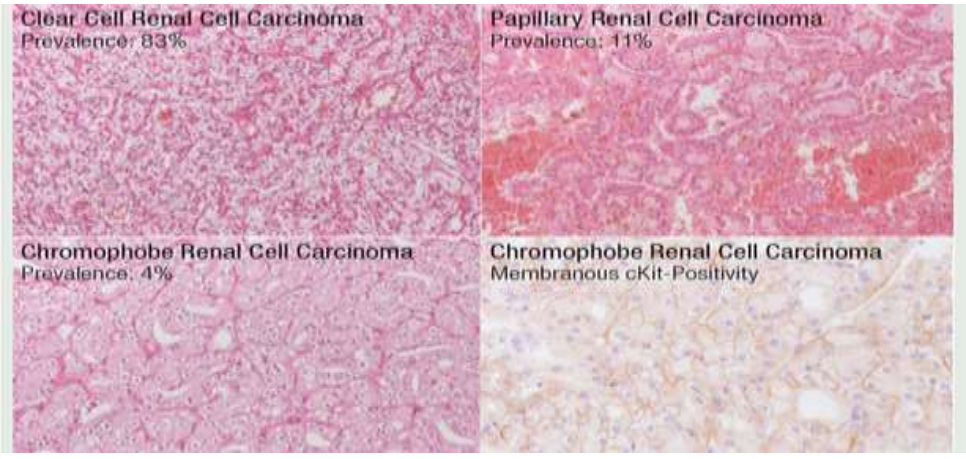



**Figure 1** : Type of Kidney Cancer[4]

Figure 2 represents the progression of kidney cancer through four stages. In Stage 1, the tumor is localized within the kidney. By Stage 2, the tumor has grown but remains confined to the kidney. Stage 3 shows the tumor spreading into nearby tissues or veins, while Stage 4 demonstrates metastasis to distant organs. This

representation highlights the critical need for accurate diagnostic tools to detect and classify kidney cancer at earlier stages.

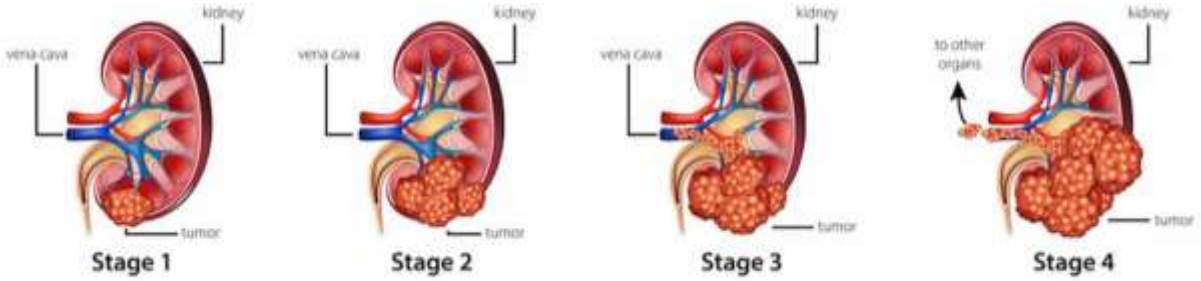



**Figure 2 :** Kidney Cancer Stages [5]

Early diagnosis can improve outcomes, while delays often necessitate invasive treatments such as nephrectomy [6]. Renal cell carcinoma (RCC) accounts for 90% of kidney cancer cases, with subtypes like clear cell, papillary, and chromophobe carcinomas posing diagnostic challenges due to their distinct histological and genetic profiles [7]. Although computed tomography (CT), magnetic resonance imaging (MRI), and ultrasound have advanced, these methods often fail to reliably differentiate between benign and malignant tumors reliably, leading to unnecessary invasive procedures [8]. Risk factors for kidney cancer include smoking, obesity, hypertension, and genetic syndromes like von Hippel-Lindau disease, with men being more frequently diagnosed than women [9]. Increased detection of incidental renal masses through widespread imaging has highlighted the need for early, precise diagnosis to improve survival rates and reduce treatment complications [10]. Advanced-stage kidney cancer is associated with poor survival rates and high medical costs, often requiring invasive procedures. Early detection, however, enables better management and minimizes the need for high-risk treatments [11]. Despite advancements, current diagnostic techniques face limitations, including variability in imaging and reliance on invasive procedures. These challenges emphasize the need for more accurate, non-invasive diagnostic methods [12]. Emerging computational methods, including artificial intelligence (AI) and machine learning (ML), offer the potential to improve diagnostic accuracy. By analyzing large datasets and identifying patterns in imaging scans, these technologies enhance early detection capabilities [13]. Furthermore, microstrip antennas provide a promising alternative for non-invasive detection by leveraging electromagnetic waves to differentiate between healthy and malignant tissues [14]. Convolutional Neural Networks (CNNs) have demonstrated significant success in tumor segmentation, classification, and feature extraction from medical imaging datasets. Pretrained models like MobileNet, EfficientNet, and SqueezeNet enhance CNN performance through transfer learning, particularly with limited domain-specific data [15, 16]. Microstrip antennas, due to their compact design and ability to operate at microwave frequencies, are increasingly being explored for medical diagnostics, including kidney cancer detection. These antennas interact with biological tissues based on their dielectric properties, The antenna properties are dielectric dependent, The dielectric properties of tissues change as there aremorphological changes in tissues due to tumor, and microstrip antenna are able to observe these changes during scanning by antennas. These scanes can be used for enabling non-invasive tumor localization and reducing the need for invasive procedures [17, 18]. Developments in antenna design, for specific resonant frequencies, have improved their sensitivity and accuracy [19].

### 1.1LITERATURE REVIEW

The diagnosis and detection of kidney-related disorders have been completely transformed by the quick developments in artificial intelligence, especially deep learning. CNNs have become essential tools for tumor segmentation, classification, and prediction when used in conjunction with hybridized models and ensemble techniques. This has improved clinical processes and increased the accuracy of diagnostics.A CNN-based system created especially for kidney tumor segmentation and the prediction was presented by Akram*et al.* A crucial need for early detection and treatment planning, their model showed excellent accuracy in defining tumor boundaries. This automated segmentation method demonstrated the effectiveness of deep learning in medical imaging by drastically reducing the need for human input [1]. Uhm *et al.* created a comprehensive deep-learning model for kidney cancer diagnosis that included multi-phase CT imaging. Their model successfully distinguished between benign and malignant kidney tumors by utilizing phase-specific characteristics, which increased diagnostic sensitivity and specificity [2]. Boundary-aware networks were established by Myronenko and Hatamizadeh in the field of 3D imaging to address issues like low contrast and noise in volumetric CT images. The potential of 3D segmentation for surgical and therapeutic planning was highlighted by their model's accurate tumor localization [3]. Gharaibeh*et al.* examined the transition from conventional machine learning to deep learning techniques,

elaborating on the function of CNNs in medical imaging. To automate kidney tumor identification and improve diagnostic accuracy, their investigation highlighted CNNs' capacity to automatically extract significant information [15]. In their investigation of semantic segmentation methods for kidney tumor identification, Abdelrahman and Viriri demonstrated how well fully automated deep learning models may lower diagnostic error and time requirements. The growing trend of using deep learning frameworks in healthcare applications is supported by their findings [16]. By combining CNNs with transformer-based topologies, including Vision Transformer (ViT) and Swin Transformer, Tanaka *et al.* expanded this field and increased the classification accuracy of kidney cancer. Their hybrid model demonstrated the promise of multi-architecture frameworks by integrating local and global feature extraction capabilities, outperforming conventional CNN-based techniques [20]. To improve tumor segmentation accuracy, Duggirala*et al.* suggested a hybrid approach that integrated fuzzy c-means clustering and support vector machines (SVM). This strategy successfully addressed the drawbacks of noisy datasets despite not being fully reliant on deep learning, demonstrating the need to combine conventional and contemporary techniques [ 21]. A 3D Multi-Scale Residual Fully Convolutional Neural Network (3D-MS-RFCNN) was presented by Yang *et al.* for the purpose of segmenting big kidney tumors. By tackling issues including irregular tumor forms and low-contrast images, this model demonstrated remarkable performance on the Kidney Tumor Segmentation Challenge (KiTS) dataset [22].To forecast chronic kidney disease (CKD) on the Internet of Medical Things (IoMT) platform, Chen *et al.* introduced an Adaptive Hybridized Deep Convolutional Neural Network (AHDCNN). This approach showed promise for widespread implementation in healthcare systems by combining multi-layered feature extraction with IoMT-based real-time analytics [23]. In order to classify kidney cancer subtypes based on miRNA genome data, Ali *et al.* used a hybrid Long Short-Term Memory (LSTM) network, highlighting the significance of combining genomic and imaging data for accurate diagnosis [24]. Ren*et al.* created a hybrid model based on Bi-LSTM that included autoencoders to predict kidney illness. Their research made clear how crucial it is to integrate structured data—like electronic health records, or EHRs—into deep learning pipelines [25]. For kidney tumor segmentation, Santini*et al*. used an ensemble multi-stage deep learning technique, which produced good accuracy on a variety of datasets. Their ensemble approach demonstrated the resilience of multi-stage frameworks in enhancing segmentation results by addressing issues like inter-patient variability and image artifacts [26]. The versatility of CNNs and hybrid architectures in treating non-cancerous kidney problems has been shown by additional research centered on the prediction of chronic kidney disease. To increase scalability and boost forecast accuracy, these techniques frequently make use of IoMT systems [27]. To improve classification performance in short datasets, Kumar *et al*. lastly investigated ensemble approaches for renal disease diagnosis by fusing CNNs with decision-tree-based classifiers [28]. The use of deep learning methods, particularly CNNs and Artificial Neural Networks (ANNs), for the early identification of kidney cancer is investigated by Rajkumar*et al.* The scientists suggest a two-pronged strategy: ANN models forecast kidney cancer based on blood test sample results, while CNNs categorize kidney images as either benign or diseased [29].This work also can be done using antennas.

Microstrip patch antennas' small size, simplicity of integration, and effective operation have made them popular for use in biomedical diagnostics. Because of these qualities, they are ideal for non-invasive medical procedures, including the diagnosis of kidney cancer. The development of good diagnostic techniques is essential to the successful treatment of kidney cancer, a serious medical condition that depends on early detection. Gayathri*et al.* demonstrated a circularly polarized microstrip patch antenna with a hexagonal shape that operates at 2.4 GHz and is intended for the detection of kidney cancer. The Rogger substrate used in this antenna had a thickness of 1.6 mm and a relative permittivity of 4.3. With a gain of 6.7 dBi and a return loss of -13 dB, the design showed excellent radiation efficiency, guaranteeing clear signal transmission. Furthermore, by guaranteeing SAR compliance a crucial safety need for biomedical applications the corporate feeding network incorporated into the architecture makes it easier to use in medical devices [30]. Islam *et al.* investigated reworking antennas to turn wireless biotelemetry systems into implantable gadgets. To provide effective in-body communication, which is essential for using antennas for medical diagnostics like kidney cancer detection, the study underlined the significance of miniaturization and optimum performance [31]. Kiourti*et al.* looked at biological telemetry using tiny implantable antennas. The study made clear how crucial it is to comply with SAR regulations and improve antenna performance in a range of biological settings[32]. To communicate with medical implants, Soontornpipit*et al.* investigated the creation of implantable microstrip antennas. To improve performance and adaptability in in-body communication systems, this study concentrated on improving size and shape, which has direct relevance to kidney cancer diagnostic instruments [33]. Lei *et al.* highlighted the benefits of circular polarization in enhancing signal stability and lowering interference when designing a circularly polarized ground radiation antenna for biomedical purposes. These results are essential for guaranteeing accurate and dependable kidney cancer detection system operation [34]. For bio-telemetry applications, Zada*et al.* created a miniature triple-band implantable antenna device that showed promise for incorporating multi-band operation with medical diagnostics. This method could make kidney cancer detection more versatile by allowing devices to function across different frequency bands [35]. Magill *et al*.

suggested an implanted, tissue-independent antenna for 2.36–2.5 GHz in-body communications. A crucial component of kidney cancer diagnostic systems, the study's emphasis on tissue independence guarantees constant performance regardless of the biological context [36]. Yang *et al.* looked at creating implantable, high-gain antennas for minimally invasive medical equipment. High-gain antennas improve signal clarity and diagnostic accuracy, according to the study. This is consistent with the high-gain properties of the hexagonal patch antenna, which make it appropriate for kidney abnormality detection [37].

### 1.2Problem Statement and Objectives

Early identification is essential for successful treatment and better patient outcomes for kidney cancer, a serious worldwide health concern. Traditional diagnostic techniques, including manually interpreting CT scans, are frequently laborious, prone to human error, and significantly rely on radiologists' skills. These drawbacks show how urgently automated technologies that increase diagnostic efficiency and accuracy are needed. Antenna design has its own set of difficulties in the field of communication technology. Compact, high-performance antennas that can continue to function reliably under a variety of operating situations are necessary for modern applications. For antenna developers, striking a balance between these demands, size restrictions, and high gain continues to be a major challenge. By offering creative solutions, this study seeks to address the issues that have been discovered in both fields. A CNN-based framework was designed to automate the classification of CT scans for kidney cancer detection, improving efficiency and accuracy while addressing problems such as low contrast in medical imaging and data variability. Concurrently, research in antenna design aims to create small, effective antenna structures with high gain to satisfy the needs of contemporary wireless communication and sensing applications. When combined, these developments aim to provide dependable and useful solutions for communication and healthcare technologies.

The present communication is divided in three sections, Section 1 introduces the background and challenges in kidney cancer detection, highlighting the potential of combining deep learning models and microstrip patch antennas. Section 2 details the materials and methodology, including the CNN-based framework for kidney tumor classification and the design and simulation of the microstrip patch antenna. Section 3 presents the results and discusses the performance of the proposed methods, including a comparison with related studies. The paper concludes by summarizing the findings and suggesting future research directions for integrating these technologies into real-world diagnostic systems.

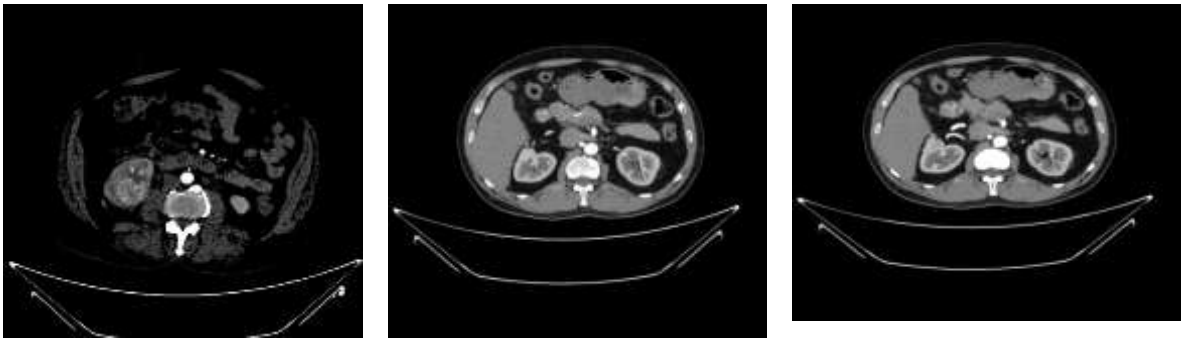
## 2Material & Methodology

### 2.1Materials

The Picture Archiving and Communication System (PACS) at several hospitals in Dhaka, Bangladesh, provided the dataset used in this investigation. CT scans of patients with kidney malignancies, cysts, normal states, or stone discoveries are included. By established procedures for CT scans of the entire abdomen and urograms, both coronal and axial cuts were chosen from contrast and non-contrast investigations. To concentrate on areas of interest, especially the kidneys, the DICOM pictures were closely examined. To protect the privacy and adhere to ethical guidelines, patient data and metadata were anonymized. The DICOM pictures were then transformed into a lossless JPG file. Each transformed image was examined by a medical technician and a radiologist to guarantee accuracy and dependability. Only the Normal and Tumor classes were used in this investigation; there were 5,077 Normal and 2,283 Tumor photos in total, for a total of 7,360 distinct images. This choice supports the study's objective of efficiently classifying kidney cancers and healthy kidneys using deep learning models.[1]



(a)



(b)

**Figure 3 :** Dataset Classes : (a) Normal , (b) Tumor

### 2.2Methodology

The proposed methodology in this research article is shown in Fig 4.

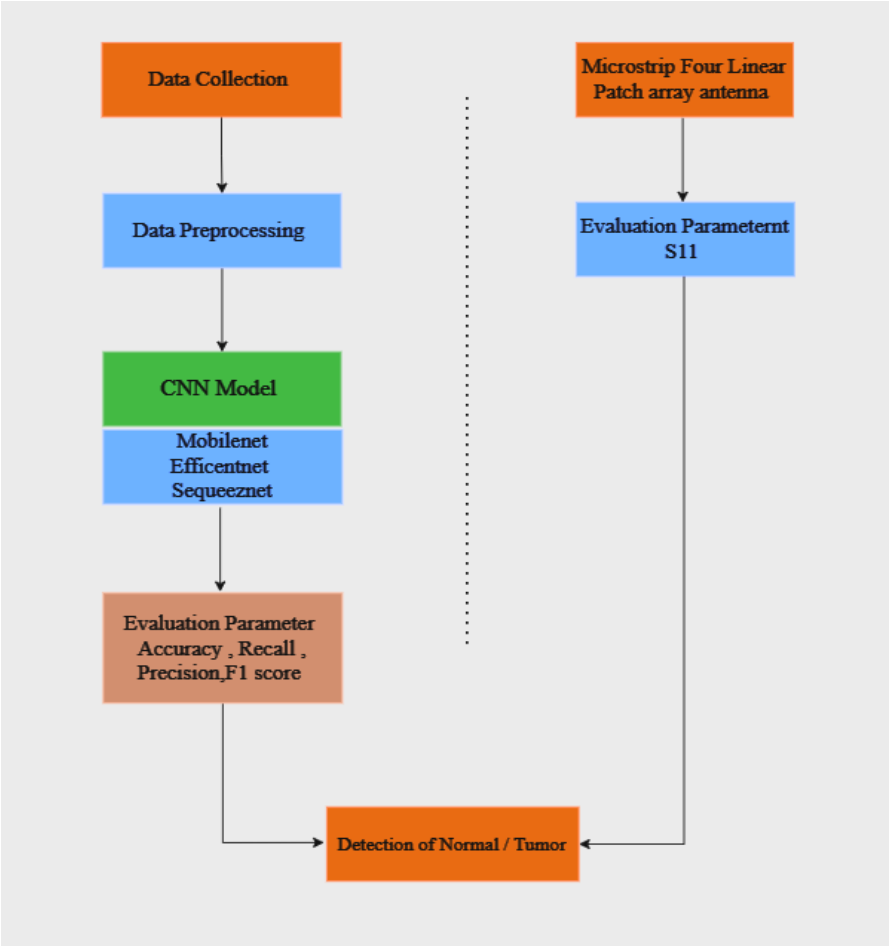



**Figure 4 : Methodology**

The data was preprocessed using different technologies like image resizing, normalization, and data augmentation. Some pre-processing techniques were used to guarantee consistency, boost generalization, and improve model performance before the dataset was used for training and assessment. To ensure that the input dimensions were consistent and appropriate for the neural network design, the first step was to resize all of the images to 150 × 150 pixels. Resizing preserved significant visual elements while standardizing image size and lowering processing demands. The pixel intensity levels were then rescaled to the [0,1] range using pixel normalization. This change is computed by Eq. (1). Faster convergence and reliable gradient updates during training are guaranteed when $X$ stands for the original pixel value.

$$X_{\{norm\}} = \frac{X - \min(X)}{\max(X) - \min(X)} \quad (1)$$

On the training dataset, data augmentation techniques were used to reduce overfitting and increase model robustness. Random rotations, shifts, zooms, shearing, and horizontal flips were among the augmentation

processes. By simulating actual fluctuations in CT images, these adjustments improve the model's ability to generalize to new data. Every augmentation procedure was expressed by Eq. (2).

$$X_{\{aug\}} = T(X) \quad (2)$$

where $X$ is the image and $T$ is the augmentation transformation applied to it. Strong model performance required a varied and improved training set, which the enlarged dataset offered. CNNs are popular for image classification tasks because of their capacity to automatically learn spatial hierarchies of information, providing the basis of the model utilized in this study. *Convolutional Layers* transform the input feature map or image using convolution techniques. The convolutional layer's filters are each made to learn a particular feature, like a texture or an edge. The convolution operation is defined as Eq. (3).

$$Y(i,j) = \sum_{m=0}^{M-1} \sum_{n=0}^{N-1} X(i+m, j+n).K(m,n) \quad (3)$$

where *Y(i, j)* is the output feature map at position $(i, j)$, *X(i, j)* is the input image or feature map at position) (i,j), *K(m,n)* is the filter/kernel applied to the input, and *M and N* are the dimensions of the filter. The input feature maps' spatial dimensions are decreased by using pooling layers. In addition to making the model invariant to little translations, this lowers the number of parameters and computations. The maximum value of the feature map is chosen in a process known as Max Pooling. To depict the pooling Eq. (4) was used.

$$Y(i,j) = \max_{m,n} X(i+m, j+n) \quad (4)$$

where, *X(i,j)* Input feature map at position (*i,j*). *Y(i,j)* Output feature map after pooling. The maximum value within the receptive field is selected to form the new feature map.To carry out classification, the output is flattened into a one-dimensional vector and then sent through fully connected layers following a number of convolutional and pooling layers. Every neuron in these layers is coupled to every other neuron in the layer above, and the result is calculated using Eq. (5).

$$y = \sigma\ (Wx + b) \quad (5)$$

Where $W$ stands for the weight matrix, $x$ for the input vector, $b$ for the bias term, and $\sigma$ for the activation function (like softmax or ReLU). In this work, pre-trained models were employed to improve model performance and cut down on training time. These models have already acquired valuable feature representations from millions of images after being pre-trained on huge datasets such as ImageNet. The pre-trained models used in this research are *MobileNetV2*, *EfficientNetB0*, and *SqueezeNet*.

*MobileNetV2* is an improved version of the original MobileNet, MobileNetV2 is intended to offer effective feature extraction with a minimal computing footprint. Performance is greatly enhanced by the model's introduction of linear bottleneck layers and inverted residuals. By employing lightweight bottleneck blocks that initially reduce the dimensionality of the data before expanding it again, the inverted residual structure aids in the preservation of significant spatial information. The final layer's linear bottleneck is special since it doesn't employ a non-linear activation function, which preserves important data. Because MobileNetV2 performs better and is more efficient at handling medical imaging tasks, it was chosen as a feature extractor in this work instead of SqueezeNet. Similar to the previous pre-trained models, MobileNetV2's top layers were eliminated, and a unique classification head was included for kidney tumor binary classification. This custom head has three layers: a dense layer with 512 units using ReLU activation, a Global Average Pooling (GAP) layer to minimize spatial dimensions, and an output layer that uses softmax to classify data into Normal and Tumor categories. With minimal computational overhead, MobileNetV2 was able to extract intricate features from the CT images thanks to its effective architecture [38].

*EfficientNetB0* a class of models called EfficientNet is made to scale effectively while using fewer parameters to achieve high accuracy. The baseline model, EfficientNetB0, uses a special compound scaling technique that scales the model's breadth, depth, and resolution consistently. EfficientNetB0 performs better than other models with fewer parameters and lower computing costs thanks to its balanced scaling strategy. To further improve its effectiveness and performance, the model makes use of swish activation and depthwise separable convolutions.EfficientNetB0 was employed as a feature extractor in this investigation. The top classification layers were eliminated, and the model was initialized using the pretrained weights from ImageNet. The model was modified for kidney tumor classification by adding a unique classification head, akin to the one utilized with MobileNetV2. EfficientNetB0 was perfect for the task at hand because it allowed for the efficient extraction of features with fewer parameters while maintaining high accuracy [39].

*SqueezeNet,* an effective deep-learning model, was created to reduce the amount of parameters while preserving excellent accuracy. The utilization of fire modules, which are made up of an expand layer and a squeeze layer, is SqueezeNet's primary characteristic. To represent the data more effectively with fewer parameters, the expand layer expands the number of output channels while the squeeze layer decreases the number of input channels. SqueezeNet's architecture enables it to perform well on image classification tasks while maintaining a modest model size. In instances where model size is important, SqueezeNet is especially helpful. Nonetheless, MobileNetV2 was selected for this study over SqueezeNet due to its enhanced feature extraction capabilities, superior handling of intricate visual patterns, and higher performance efficiency, especially for the kidney tumor classification assignment [40].

Two optimization methods, Adam (Adaptive Moment Estimation) and SGD (Stochastic Gradient Descent), were used to train the CNN model. The effectiveness of both optimizers in reaching effective convergence during training was evaluated. Adam uses estimates of the gradients' first and second moments to calculate adaptive learning rates for each parameter. Eq. (6) represents the Adam guidelines.

$$\theta_t = \theta_{t-1} - \left(\frac{\eta}{\sqrt{v_t} + \epsilon}\right).m_t \qquad (6)$$

where $m_t$ is thebias-corrected first-moment estimate, $v_t$ is thebias-corrected second-moment estimate of $m_t$. Mini-batches of data are used by SGD to update the model's parameters, adding noise to the optimization process to assist in preventing local minima. The SGD rule is shown by Eq. (7).

$$\theta_t = \theta_{t-1} - \eta \cdot \nabla_\theta J(\theta_{t-1}) \qquad (7)$$

where $\theta_t$ is the parameter at iteration $t$ , $\eta$ is the Learning rate (step size), and $\nabla_\theta J(\theta_{t-1})$ is the gradient of the loss function

The dataset was split using an 80-10-10 split ratio into training, validation, and test sets in order to assess the performance of the CNN architectures (MobileNetV2, EfficientNetB0, and SqueezeNet). This preserved enough data for testing and training while guaranteeing a fair evaluation. The training process began with initializing all models using pre-trained weights from ImageNet. The top layers of these models were replaced with a custom classification head designed for the binary classification task of identifying Normal and Tumor cases. The categorical cross-entropy loss function was used to measure the difference between predicted and actual class probabilities. Both Adam and SGD optimizers were tested with an initial learning rate of 0.001, and a dynamic learning rate scheduler adjusted the learning rates based on validation loss improvements. To ensure computational efficiency and stability, a batch size of 32 was used during training. The models were trained for 20 epochs, with early stopping implemented to prevent overfitting. During training, validation loss and accuracy were monitored after each epoch. The model checkpoint technique was applied to save the model with the best validation performance. Data augmentation techniques such as rotations, zooming, and flipping were applied to enhance generalization and robustness. To visualize the true positive, true negative, false positive, and false negative predictions, a confusion matrix is used.

**Confusion Matrix**

| | **Predicted Positive** | **Predicted Negative** |
|---|---|---|
| **Actual Positive** | True Positive (TP) | False Negative (FN) |
| **Actual Negative** | False Positive (FP) | True Negative (TN) |

True Positive (TP) the model correctly predicted the positive class. False Negative (FN) the model predicted the negative class but the actual class is positive. False Positive (FP) The model predicted the positive class but the actual class is negative. True Negative (TN) The model correctly predicted the negative class. With the help of CM, the following metrics were computed on the validation and test sets to compare the models.

**Accuracy**is to measure the overall performance of the models and is expressed by Eq. (8).

$$Accuracy = \frac{(TP + TN)}{TP + TN + FP + FN} \qquad (8)$$

**Precision** is to evaluate the ratio of true positive predictions to total positive predictions and is expressed by Eq. (9).

$$Precision = \frac{TP}{TP + FP} \qquad (9)$$

**Recall (sensitivity)**is to assess the ability of the model to correctly identify true positive samples and is expressed by Eq. (10).

$$Recall = \frac{TP}{TP + FN} \qquad (10)$$

**F1-Score** provides a harmonic mean of precision and recall, particularly useful in imbalanced datasets, and is expressed by Eq. (11).

$$F1 - Score = 2.\frac{Precision.Recall}{Precision + Recall} \quad (11)$$

A crucial step in maximizing the effectiveness of machine learning models is hyperparameter tuning. It entails methodically identifying the optimal set of hyperparameters to optimize model performance while minimizing the loss function. The size of the steps taken during gradient descent is controlled by the learning rate (η). While a larger learning rate expedites training but runs the danger of exceeding the minimum, a lower learning rate guarantees stability but may impede convergence. During training, the term "epochs" describes how many times the complete dataset is run through the model. The model's ability to learn intricate patterns is directly impacted by changes to the depth (number of layers) and width (number of units per layer).

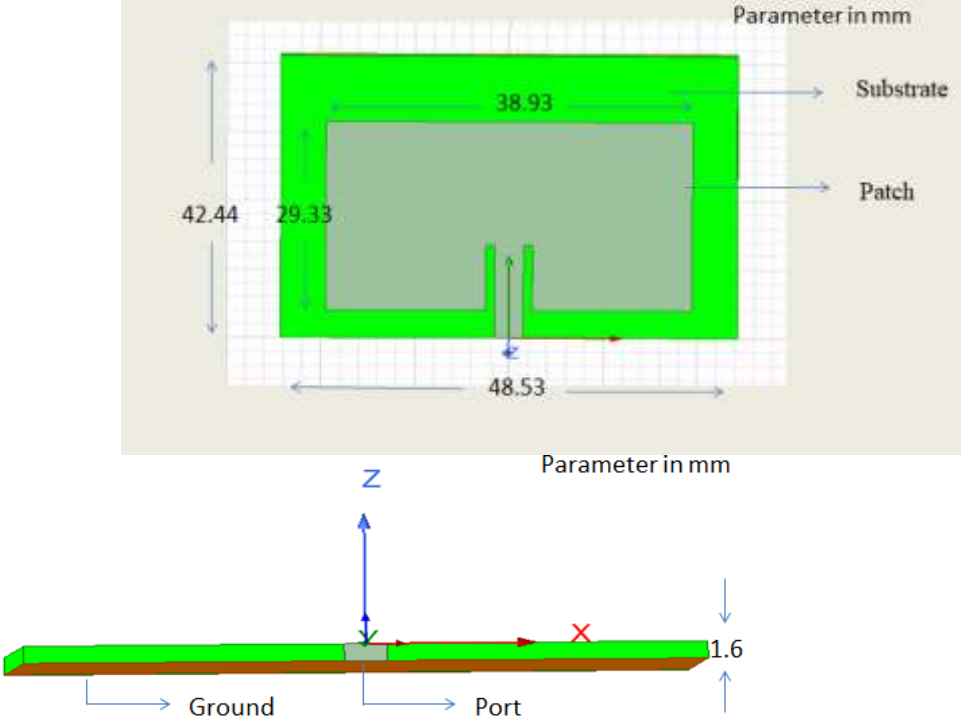



**Figure 5**: **Microstrip Patch Antenna Design**
*Alabeled diagram of the antenna, showing the dimensions*

Figure 5 demonstrates the detailed design of the microstrip patch antenna. A microstrip patch antenna intended for use in kidney cancer detection applications operating at 2.4 GHz is one of the materials used in this investigation. The antenna is designed using an FR4 substrate with Relative Permittivity of 4.4, Loss Tangent of 0.02, and Thickness of 1.6 mm. The choice of FR4 was driven by its widespread availability, cost-effectiveness, and suitability for prototyping purposes. The patch and ground plane were fabricated using copper, ensuring excellent conductivity and efficient radiation performance. The dimensions of the microstrip patch antenna are considered as Width of Patch as 36.78 mm, Length of Patch as 28.26 mm, Width of Ground as 46.38 mm, Length of Ground as 41.22 mm, Width of Feed as 3.045 mm, and Length of Feed as 13.47 mm.

At 2.4 GHz, a renal system phantom will also be created in the future to mimic the dielectric characteristics of human tissues. The phantom will consist of multiple layers representing different tissues, including the kidney cortex, renal capsule, muscle, fat, and skin, to evaluate the antenna's performance in realistic conditions. The antenna is specifically designed to operate at 2.4 GHz, a frequency commonly used in medical applications due to its ability to penetrate human tissues. The antenna substrate ensures a balance between structural rigidity, affordability, and acceptable high-frequency performance. The dimensions of the antenna components were calculated and optimized using standard microstrip patch antenna design formulas to achieve resonance at 2.4 GHz, ensuring effective performance at the target frequency. The antenna design was modeled and simulated using the High-Frequency Structure Simulator (HFSS), a

commercial electromagnetic simulation software. The simulation enabled the calculation of return loss, radiation pattern, and impedance matching at the operating frequency of 2.4 GHz. The antenna was optimized to achieve a return loss below -10 dB, ensuring high radiation efficiency and minimal signal reflection. The patch dimensions, substrate thickness, and feed length were adjusted in the simulation to ensure efficient radiation, making the antenna well-suited for kidney cancer detection applications. Algorithm 1 shows the proposed methodology.

**Algorithm 1**
**Start**
**Input :** CT scan images of kidneys
**Output: Cancer detection**

1. Collection of CT scan images of kidneys,
2. Preprocess by resizing to 150 × 150 pixels, normalize to [0,1], and augment with rotations, flips, and zooms.
3. Splitting the dataset into 80% training, 10% validation, and 10% testing subsets.
4. Selection of pretrained models (MobileNetV2, EfficientNetB0, SqueezeNet), modify by replacing the classification layers with a dense layer, GAP layer, and softmax output.
5. Training of models using Adam and SGD optimizers with a batch size of 32, dynamic learning rates, and early stopping over a maximum of 20 epochs.
6. Evaluation of model performance using Accuracy, Precision, Recall, F1-Score, and AUC metrics, along with a confusion matrix analysis.
7. Design a 2.4 GHz microstrip patch antenna using FR4 substrate, optimize in HFSS to achieve S11<−10 dB, VSWR ≈ 1.1, and a gain of 3.43 dB.
8. Use the deep learning models to classify kidney tumors from CT images and the microstrip patch antenna for electromagnetic sensing to detect abnormalities independently.

## 3. Results and Discussion

The performance of various models, including pre-trained models like MobileNetV2, EfficientNetB0, and SqueezeNet, (CNN) trained with Adam and SGD optimizers, was assessed in this study for the kidney tumor classification problem. The models were trained to categorize the datasets that were tagged as Normal and Tumor. Accuracy, precision, recall, F1-score, and Area under the Curve (AUC) were among the measures used to evaluate the performance. These metrics offer a thorough grasp of the model's capacity to manage unbalanced input, categorize the images effectively, and strike a balance between false positives and false negatives. Table 1 summarizes the findings and displays each model's F1-score.

**Table 1: Model Performance Comparison**

| Model | F1-Score (%) |
|---|---|
| CNN (Adam) | 95.75 |
| CNN (SGD) | 92.45 |
| MobileNetV2 | 97.04 |
| EfficientNetB0 | 82.00 |
| SqueezeNet | 96.51 |

Table 1 shows the performance of various deep learning methods in the field of kidney tumor classification on CT images in terms of F1-scores. In every model, MobileNetV2 gave the best F1-score of 97.04% which shows the best classification performance. SqueezeNet also achieved a good performance (96.51%). The CNN model trained with the Adam optimizer outperforms the CNN model trained with the SGD optimizer by 95.75% and 92.45% respectively which shows that the CNN model with the Adam optimizer has a better optimization capability. The best performance was obtained by EfficientNetB0 with the F1-score of 82.00%. The overall results showed that pre-trained transfer learning models are effective in accurate detection of the kidney tumor with excellent performance. Figure 6 presents the Receiver Operating Characteristic (ROC) curve for each model, including Adam, SGD, MobileNetV2, EfficientNetB0, and SqueezeNet, highlighting their respective areas under the curve (AUC).

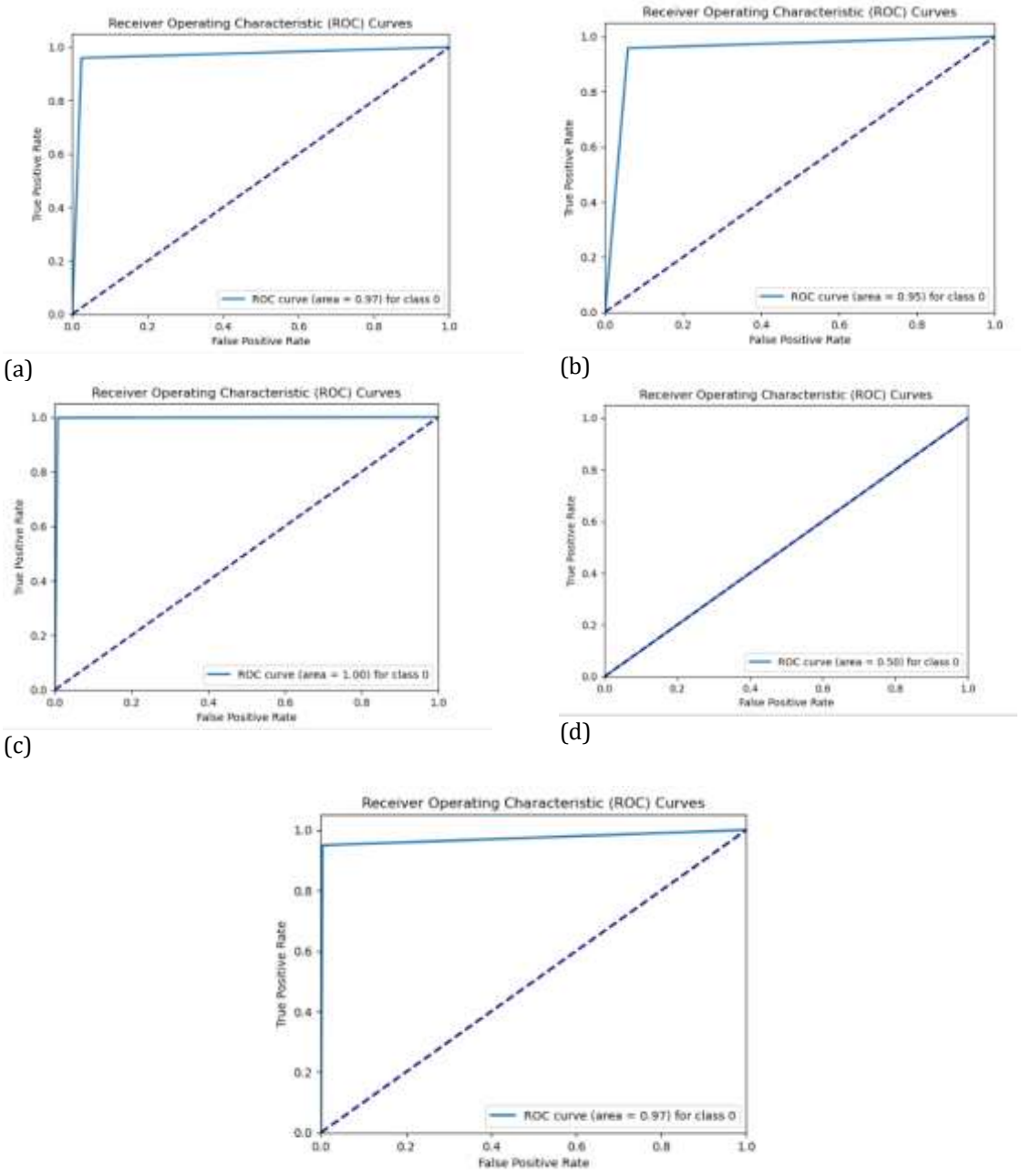



**Figure :6** ROC curve with area (a) CNN (Adam) , (b) CNN (SGD) , (c) MobileNetV2 , (d) EfficientNetB0 , (e) SqueezeNet

Using CNN with the Adam optimizer, the authors attained 97.84% accuracy, 95.30% precision, 96.22% recall, and 95.75% F1-score. The CNN model trained using the Adam optimizer demonstrated strong performance in kidney tumor classification and false positive reduction. With a precision of 95.30%, the model is reliable in detecting tumor instances with few false positives. With a recall of 96.22%, the model was able to correctly identify a significant percentage of true tumors. This is crucial because identifying as many true positive cases as possible is critical in medical diagnosis. The model's overall efficacy is reflected in the F1-score, which strikes a balance between precision and recall. The model's remarkable ability to differentiate between the Normal and Tumor classes is further supported by the AUC of 0.97. The model can converge rapidly and achieve high performance in fewer epochs due to the adaptive learning rate of the Adam optimizer. The CNN design may have succeeded in this task because of its layered nature, which allowed it to capture the spatial hierarchies in the images. As compared to the Adam-based model, the CNN model trained using the SGD optimizer performed less effectively overall. Its accuracy was 91.29%, recall was 96.72%, and F1-score was 92.45% and AUC was 0.95. However, its precision of 88.35% was noticeably lower than that of the Adam optimizer. This suggests that although the model performs well in detecting tumors, it frequently generates more false positives. SGD's stochastic nature may be the source of the decreased precision, as it forces the model to make more frequent updates during learning, which could result in more classification errors. Despite its widespread use due to simplicity and ability to avoid local

minima, the comparatively lower performance of SGD indicates that the Adam optimizer is a better choice for pretrained models, particularly for tasks requiring higher precision and reliability, such as tumor detection. With an F1-score of 97.04%, 98.49% accuracy, and 99.00% precision, the pretrained MobileNetV2 model demonstrated remarkable performance. The high precision indicates that there were few false positives, and the model was quite accurate in recognizing tumor images. A large number of tumor cases were correctly identified by MobileNetV2, as evidenced by its excellent recall of 95.24%. Because MobileNetV2 was pretrained on the extensive ImageNet dataset, it illustrated the advantages of transfer learning. The model was a very good choice because it could generalize to new tasks, like kidney tumor detection, without requiring extensive training on a small dataset. Additionally, the model's outstanding discriminative performance is demonstrated by its AUC of 1, underscoring its applicability for medical imaging applications. The kidney tumor dataset showed poor performance from EfficientNetB0, a state-of-the-art model, with an accuracy of 69.80% and an F1-score of 82.00%. With 100% recall and just 69.80% precision, the model's performance was noticeably unbalanced. This finding suggests that EfficientNetB0 produced a high percentage of false positives for the Tumor class due to its bias toward predicting the Normal class. The model did no better than random guessing, according to the AUC of 0.50. The model's intrinsic complexity and the challenge of adapting it to a limited dataset are two of the reasons for this subpar performance. EfficientNetB0's design might have had trouble adjusting to the simple kidney dataset, despite being typically effective for large, diverse datasets. SqueezeNet performed admirably, matching MobileNetV2 in terms of accuracy (98.15%) and F1-score (96.51%). With 97.60% precision and 95.45% recall, the model demonstrated good performance in distinguishing between the Normal and Tumor classes. The outstanding discriminative capacity is also indicated by the AUC of 0.97. Similar to MobileNetV2, SqueezeNet's effective architecture, which is made to be lightweight while maintaining high accuracy, proved advantageous. Smaller models like SqueezeNet can also perform well in medical image dataset classification tasks, especially where computing efficiency is crucial, as demonstrated by doing almost as well as MobileNetV2.

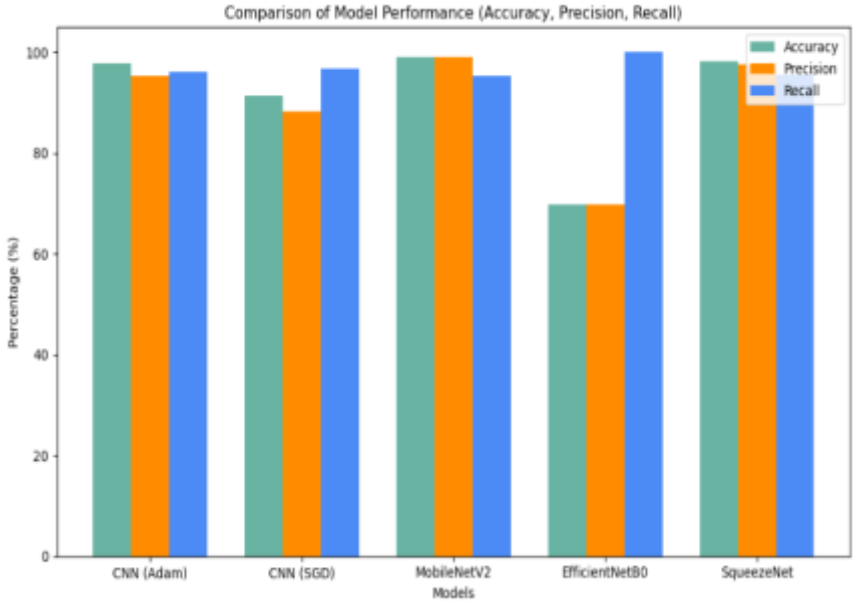



**Figure 7:** Comparison of model performance (Accuracy , Precision, Recall)

The deep learning models, especially the MobileNetV2, showed great performance in detecting kidney tumors; however, the microstrip patch antenna has an important role in this proposed non-invasive diagnostic system for reliable transmission. Thus, in the study, the design and performance analysis of a micro strip patch antenna at 2.4 GHz for the application of tumor detection using electromagnetic wave is taken into consideration. The simulated S11 parameter of the proposed antenna is shown in figure 8. S11 parameter (reflection coefficient) was used to examine the antenna's impedance matching and transmission qualities. The S11 value is lower in this case, signifying less signal reflection and better power transfer, demonstrating the antenna's effectiveness for biomedical sensing and communication applications.

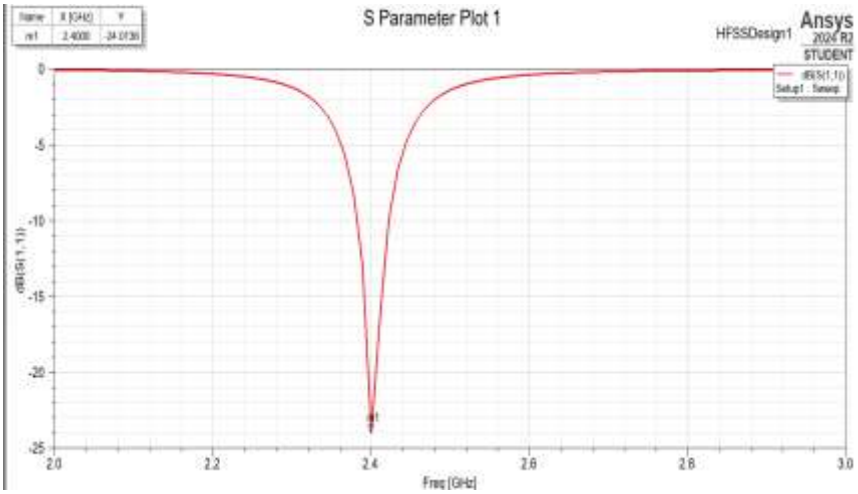



**Figure 8 :**Simulated S11Parameter of the Microstrip Patch Antenna at 2.4 GHz

At the target frequency of 2.4 GHz, the S11 value was measured to be -24.0136 dB. This result indicates excellent impedance matching, as values below -10 dB are generally considered acceptable for most applications. The significantly lower S11 value demonstrates minimal power reflection, ensuring efficient transmission and reception of signals. The optimized design of the patch, FR4 substrate, and feed line contributed to the improved performance. By carefully selecting the FR4 substrate material and optimizing the antenna dimensions, the desired resonant frequency and efficient operation were achieved. This level of performance establishes the proposed antenna as a suitable candidate for non-invasive kidney cancer detection applications. Further work involve the validation of these results through experimental testing and analyzing the antenna's performance in a realistic tissue phantom environment. The Voltage Standing Wave Ratio (VSWR) is an important parameter that indicates the efficiency of power transfer from the antenna to free space. A lower VSWR value closer to 1 is desirable, as it demonstrates minimal signal reflection and better impedance matching. Figure 9 shows the VSWR plot of the proposed microstrip patch antenna. At the target frequency of 2.4 GHz, the VSWR value is approximately 1.0958, which is significantly below the acceptable threshold of 2.

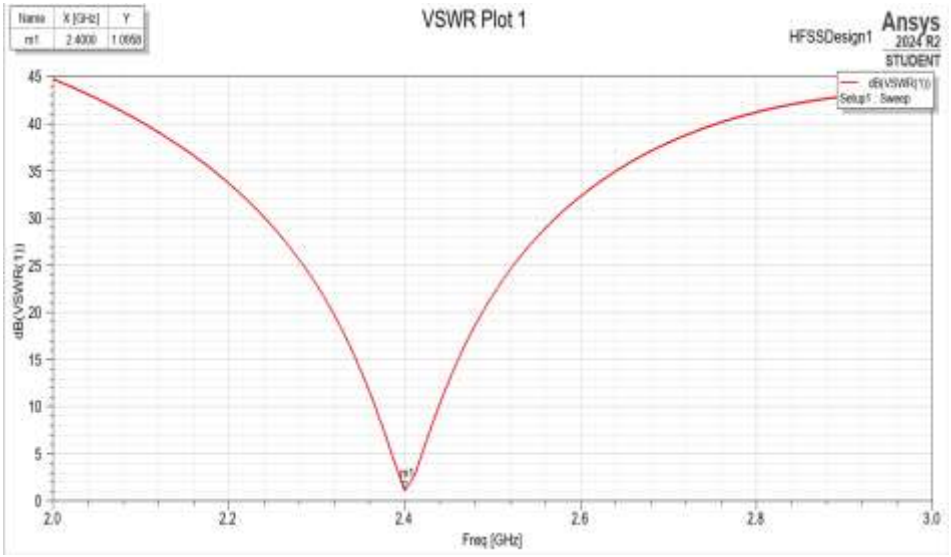



**Figure 9 :**VSWR plot of the proposed microstrip patch antenna

The results obtained are consistent with the proposed microstrip patch antenna for 2.4 GHz of high impedance matching to obtain efficient radiations characteristics and minimum power loss during signal transmission. The significant drop in the VSWR curve around 2.4 GHz suggests that the antenna dimensions and substrate parameters have been carefully tuned for optimal performance. The transmission of such efficient electromagnetic signals is crucial to accurately detect changes in the dielectric properties of the kidney tissues corresponding to cancerous tumors. Thus, the proposed antenna system would be able to provide reliable electromagnetic sensing, and enhance the accuracy of detection for kidney cancer without invasive procedures.

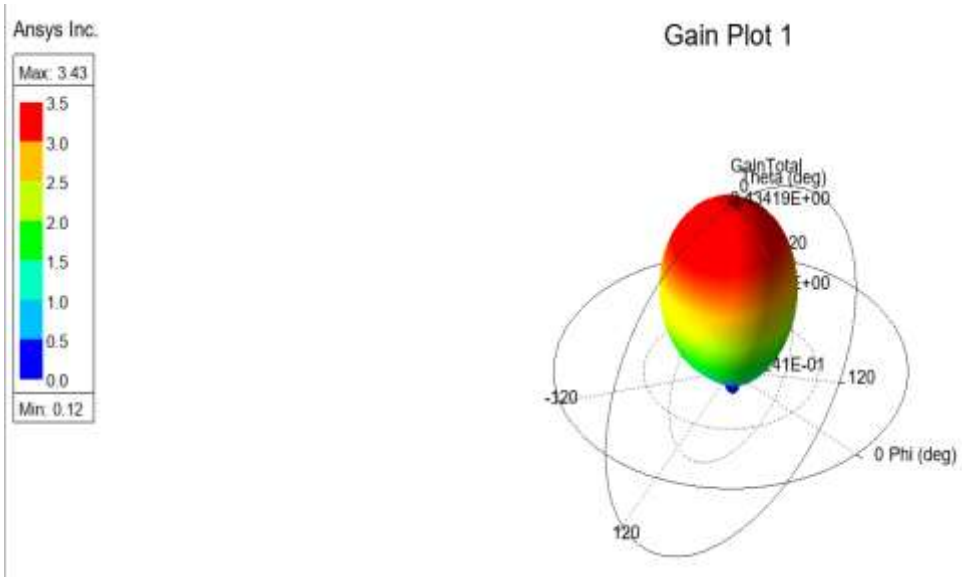



**Figure 10 :**3D Gain plot of the proposed microstrip patch antenna

The gain characteristics of the proposed microstrip patch antenna are represented by the direction and strength of the electromagnetic radiation in space as shown in the 3D radiation pattern in Figure 10. The antenna has a maximum gain of ~3.43 dB, showing a focused and stable radiation pattern ideal for targeted biomedical sensing applications. Directional radiation is important as it helps to increase the accuracy of the interaction of electromagnetic radiation with kidney tissues, thus increasing the reliability of non-invasive kidney cancer detection. The radiation performance obtained is good enough to show that the antenna design is effective for medical imaging and diagnostic applications. The designed layout of Microstrip patch antenna for fabrication is shown in the figure 11.

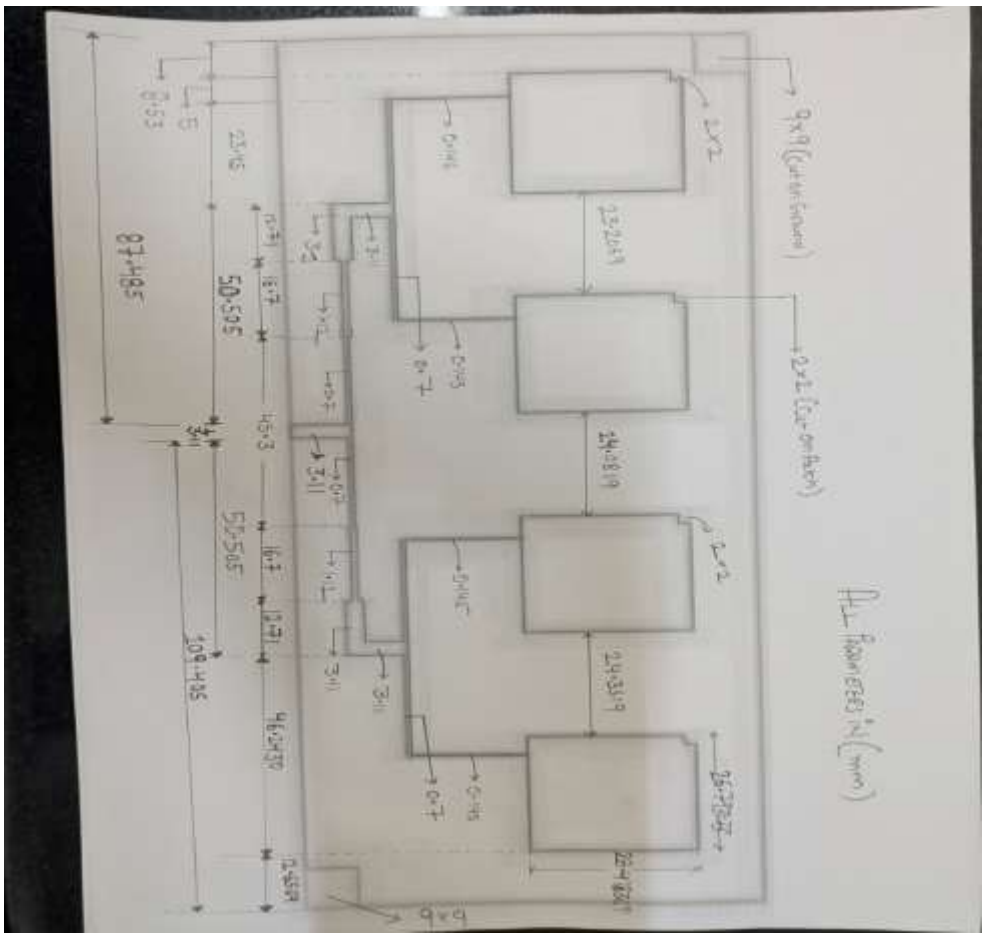


**Figure 11** Design For antenna Fabrication

The detailed designs and dimensional parameters of the proposed micro strip patch antenna for fabrication and biomedical sensing is shown in Fig. 11. The antenna structure is made up of multiple rectangular radiating patches which are linked through microstrip feed lines on a dielectric substrate. Dimensions are given in millimetres which will be necessary for accurate fabrication and operational performance at the target frequency of 2.4 GHz. Each patch's size and the spacing of the feed elements have been carefully optimized to ensure good impedance matching, current stability and effective electromagnetic radiation. The dimensions of the ground plane and cut parts are also shown to reduce reflection from the ground surface and improve the performance of the antenna. The symmetrical distribution of the patch elements helps to achieve better radiation characteristics and directivity gain. This fabricated antenna configuration is designed specifically for the non-invasive detection of kidney cancer, where it is important to have efficient propagation of electromagnetic waves and correct sensing of variations in the dielectric properties of kidney tissues, for reliable tumor identification.

## 4. Comparison of work

**4.1 Comparison of proposed work with same Dataset :** K. Rajkumar *et al.* used a CNN model to classify kidney cancer images, achieving a validation accuracy of 99.6% and a training accuracy of 96.4%. In contrast, this study incorporates pretrained models like MobileNetV2, EfficientNetB0, and SqueezeNet alongside a custom CNN. The pretrained models demonstrated significant advantages in terms of robustness and precision, particularly for smaller datasets, outperforming the standalone CNN in overall performance. MobileNetV2 and SqueezeNet achieved validation accuracies of 99.0% and 98.15%, respectively, while EfficientNetB0 showed relatively lower performance with a validation accuracy of 69.8%. These results highlight the potential benefits of transfer learning over standalone CNNs in handling complex classification tasks. Figure 12 shows the comparison with the same dataset.

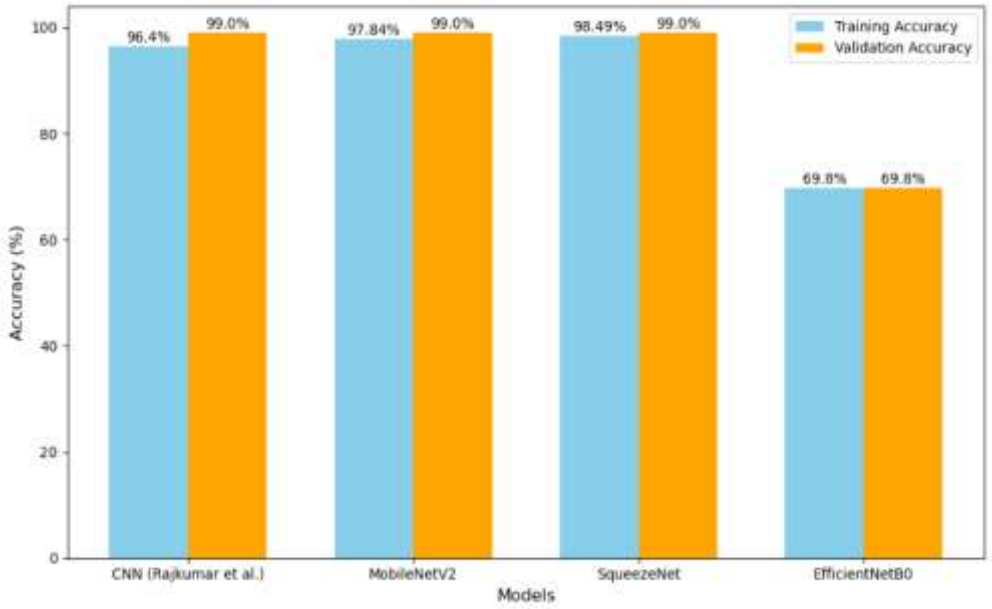



**Figure 12 :** comparison with same dataset

The presented results highlight the performance of various models using the same dataset. MobileNetV2 and SqueezeNet achieved remarkable accuracy and precision, showcasing their robustness in tumor classification tasks. These models benefited significantly from transfer learning, enabling efficient generalization despite the limited dataset size. EfficientNetB0, however, struggled with balance and precision, emphasizing the challenges associated with adapting complex architectures to smaller, specialized datasets. These outcomes underline the critical role of model selection in achieving optimal performance for medical imaging tasks.

**4.2 Comparison of proposed work with other dataset :** M. Pavithra and B.T. Geetha utilized Radial Basis Function Support Vector Machine (RBF SVM) and Random Forest (RF) classifiers for chronic kidney cancer detection using a dataset of 280 samples collected from the Vermont Center for Ecostudies (VCE) repository. Their study achieved impressive results, with RBF SVM attaining an accuracy of 99.0% and Random Forest achieving 98.0% accuracy. Similarly, this study applied pretrained deep learning models to classify kidney cancer using a different dataset, achieving comparable results. MobileNetV2 achieved 99.0% accuracy, matching the performance of the RBF SVM. SqueezeNet achieved an accuracy of 98.0%, similar to the Random Forest model, while EfficientNetB0 demonstrated significantly lower performance at 69.8%,

reflecting its challenges with smaller datasets. Figure 13 shows the comparison of these results with other datasets [41].

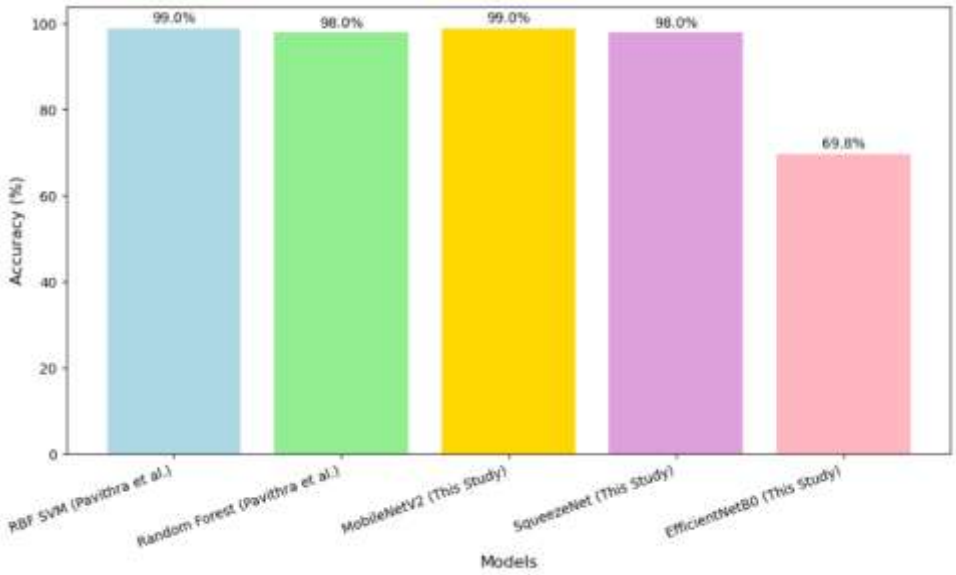



**Figure 13 :**Comparison with other dataset

The results demonstrate that MobileNetV2 and SqueezeNet achieve comparable performance to traditional machine learning models like RBF SVM and Random Forest on a different dataset, while EfficientNetB0 falls short due to its challenges with smaller datasets. The consistent high accuracy of MobileNetV2 and SqueezeNet emphasizes the robustness and adaptability of these architectures for kidney cancer detection tasks.In comparison, the classical models RBF SVM and Random Forest highlight the potential of non-deep-learning-based approaches, but they lack the scalability and feature extraction capabilities of deep learning models. This underscores the advantage of utilizing pretrained architectures for medical imaging, where data quality and diversity are often limited.

**4.3 Comparison of Antenna results :**The study by Gayathri et al. proposed a circularly polarized hexagonal microstrip patch antenna for kidney cancer detection, operating at 2.4 GHz. Utilizing a Rogers substrate with a relative permittivity of 4.3 and a thickness of 1.6 mm, their antenna achieved a return loss (S11) of -13 dB and a gain of 6.7 dB. The design emphasized compactness, efficient radiation, and compliance with specific absorption rate (SAR) safety limits.In contrast, our study developed a microstrip patch antenna operating at 2.4 GHz using an FR4 substrate with a relative permittivity of 4.4, a loss tangent of 0.02, and a thickness of 1.6 mm. The proposed antenna achieved a return loss (S11) of -24.0136 dB, significantly better than the -13 dB reported by Gayathri et al., indicating superior impedance matching and minimal signal reflection. Additionally, our antenna's maximum gain was 3.43 dB, which, while lower than the 6.7 dB of Gayathri et al.'s design, still provides effective signal transmission for non-invasive kidney cancer diagnostics.Both designs prioritize compactness and ease of integration. However, Gayathri et al. focused on circular polarization, achieving an axial ratio of 0.8 dB, which enhances signal stability and reduces interference. Our design, on the other hand, emphasizes optimizing return loss and VSWR, achieving a VSWR of approximately 1.0958, compared to the 1.09 reported in their study, reflecting a similar level of impedance matching efficiency. While Gayathri et al. utilized specific slot designs within the patch to enhance radiation efficiency, our design optimized the patch dimensions and feed length for resonance at 2.4 GHz. This approach ensured efficient operation and bandwidth optimization, making the antenna suitable for medical diagnostics [30].

## 5. Conclusion and Future work

The study evaluates the performance of deep learning models and microstrip patch antenna designs in the context of kidney cancer detection, highlighting the synergy between advanced computational techniques and electromagnetic sensing methods. The results provide critical insights into the capabilities and limitations of each approach, emphasizing their contributions to non-invasive diagnostics and medical imaging technologies. In the deep learning segment, pretrained architectures such as MobileNetV2 and SqueezeNet demonstrated remarkable accuracy and efficiency, achieving 99.0% and 98.15% accuracy, respectively. These models highlight the potential of transfer learning to overcome the challenges posed by limited datasets, enabling robust generalization and effective tumor classification. Conversely, EfficientNetB0 underperformed with an accuracy of 69.8%, showcasing the difficulties in adapting complex

models to specialized, small-scale datasets. This underscores the importance of selecting model architectures that align with the dataset characteristics and application requirements. The CNN model trained with the Adam optimizer performed exceptionally well, achieving 97.84% accuracy, showcasing the optimizer's adaptability in rapidly converging to high-performance solutions. In contrast, the CNN model trained with SGD exhibited a lower accuracy of 91.29%, highlighting its stochastic nature, which can lead to reduced precision due to frequent parameter updates. These findings indicate that optimizing training strategies is critical for enhancing diagnostic accuracy in medical imaging tasks.The microstrip patch antenna, designed to operate at 2.4 GHz, demonstrated excellent impedance matching and minimal signal reflection, as evidenced by an S11 parameter of -24 dB and a VSWR of approximately 1.0958. These results validate the antenna's suitability for non-invasive diagnostic applications, providing a foundation for integrating electromagnetic sensing into kidney cancer detection systems. The maximum gain of 3.43 dB and the well-focused radiation pattern further emphasize the antenna's effectiveness in targeted medical applications. When compared to similar studies, such as Gayathri*et al.*, the proposed antenna design excels in minimizing return loss while maintaining efficient performance, despite slightly lower gain values. By combining these methodologies, the study establishes a comprehensive framework for advancing kidney cancer diagnostics. Deep learning models offer precise and automated classification, while microstrip antennas provide non-invasive, real-time electromagnetic sensing capabilities. Together, they address the limitations of traditional imaging methods, reducing the need for invasive procedures and enhancing patient outcomes. Future work will involve experimental validation of the proposed antenna design using realistic tissue phantoms to ensure accurate performance in clinical settings. Additionally, further optimization of deep learning models through hybrid architectures and the incorporation of additional data sources, such as genomic information, can enhance diagnostic accuracy and robustness. These developments promise a significant leap forward in integrating technology with healthcare for effective and early kidney cancer detection.

**Declarations**

**ETHICS APPROVAL AND CONSENT TO PARTICIPATE**:Not applicable
**HUMAN AND ANIMAL RIGHTS**:No humans were used for the studies that are the basis of this research.
**CONSENT FOR PUBLICATION**: Not applicable.
**Availability of data and materials**: The data and supportive information are available within the article.
**Funding**: Authors declare no funding for this research
**Conflicts of interest:** The authors declare that they have no conflict of interest
**Acknowledgments:** Declared none.
**Clinical trial number:** not applicable
**Usage of AI tool** : Only Quillbolt and Grammarly was used for English language.
**Author contribution**: All authors contributed equally to this work. The first author was responsible for conceptualization, methodology development, algorithm implementation, experimentation, and initial manuscript drafting. The second author contributed to data analysis, validation, result interpretation, critical revision of the manuscript, and overall supervision. Third author help in working of Anteena part. All authors reviewed and approved the final manuscript.

## References

[1] Z. Akram, M. S. Kareem, B. Mughal, Z. Ahmed, and S. Aziz, “Cancerous Tumor Segmentation of Kidney Images and Prediction of Tumor Using Medical Image Segmentation and Deep Learning Techniques,” in *Proceedings of the 7th International Conference on Trends in Electronics and Informatics (ICOEI 2023)*, 2023, pp. 1197–1202.

[2] K.-H. Uhm, S.-W. Jung, M. H. Choi, H.-K. Shin, J.-I. Yoo, S. W. Oh, J. Y. Kim, H. G. Kim, Y. J. Lee, S. Y. Youn, S.-H. Hong, and S.-J. Ko, “Deep learning for end-to-end kidney cancer diagnosis on multi-phase abdominal computed tomography,” in *Proceedings of the 7th International Conference on Trends in Electronics and Informatics (ICOEI 2023)*, 2023, pp. 1197–1202.

[3] A. Myronenko and A. Hatamizadeh, “3D kidneys and kidney tumor semantic segmentation using boundary-aware networks,” in *Proceedings of the 7th International Conference on Trends in Electronics and Informatics (ICOEI 2023)*, 2023, pp. 1197–1202.

[4] Genitourinary Tract Tumours | OncologyPRO

[5] Diagram Showing Different Stages Kidney Cancer Stock Vector (Royalty Free) 1032050758 | Shutterstock

[6] R. L. Siegel, K. D. Miller, and A. Jemal, "Cancer statistics, 2020," *CA: A Cancer Journal for Clinicians*, vol. 70, no. 1, pp. 7–30, Jan. 2020.

[7] S. Padala, D. A. Barsouk, A. Thandra, et al., "Epidemiology of renal cell carcinoma," *World Journal of Oncology*, vol. 11, no. 3, pp. 79–87, 2020.

[8] J. Hsieh, A. White, M. Shah, et al., "Imaging in kidney cancer: A review of radiologic modalities and imaging algorithms," *Journal of Clinical Oncology*, vol. 38, no. 7, pp. 658–667, Mar. 2020.

[9] American Cancer Society. *Cancer Facts & Figures 2024*. Atlanta: American Cancer Society; 2024.
[10] M. A. Linehan, W. M. Walther, and R. L. Zbar, "The genetic basis of kidney cancer: A metabolic disease," *Nature Reviews Urology*, vol. 7, no. 5, pp. 277–285, May 2010.
[11] A. Subasi, et al., "Epileptic seizure detection using hybrid machine learning methods," *Neural Computation & Applications*, 2019.
[12] J. Kim, H. Lee, et al., "Deep learning in medical imaging: Current trends and future prospects," *Journal of Clinical Imaging Science*, vol. 8, no. 2, pp. 63–75, 2021.
[13] Z. Liu, Y. Xie, et al., "The application of microstrip antennas in medical imaging and tumor detection," *IEEE Transactions on Biomedical Engineering*, vol. 68, no. 4, pp. 1210–1218, Apr. 2021.
[14] A. K. Gupta, et al., "Artificial intelligence and machine learning in early detection of kidney cancer: A review," *Journal of Urological Research*, vol. 48, no. 3, pp. 200–210, 2022.
[15] M. Gharaibeh, D. Alz'bi, M. Abdullah, I. Hmeidi, and M. R. A. Nasar, "Radiology Imaging Scans for Early Diagnosis of Kidney Tumors: A Review of Data Analytics-Based Machine Learning and Deep Learning Approaches," in *Proceedings of the 7th International Conference on Trends in Electronics and Informatics (ICOEI 2023)*, 2023, pp. 1197–1202.
[16] A. Abdelrahman and S. Viriri, "Kidney Tumor Semantic Segmentation Using Deep Learning: A Survey of State-of-the-Art," *MDPI Journal of Imaging*, vol. 8, no. 3, pp. 55, 2022.
[17] Shahzad, A., Khan, M. A., Iqbal, J., et al., "Wearable microstrip patch antenna design for non-invasive breast cancer detection," *Sensors*, vol. 19, no. 16, pp. 3371, 2019.
[18] Ahirwar, S., "Microwave imaging for tumor detection: An overview," *International Journal of Biomedical Imaging*, vol. 2021, pp. 1-10, 2021.
[19] Zhang, Q., Sun, W., Yang, Y., "Advances in microstrip antennas for medical applications," *IEEE Transactions on Antennas and Propagation*, vol. 67, no. 8, pp. 5141-5154, 2019.
[20] T. Tanaka, Y. Yamamoto, S. Nakamura, H. Suzuki, and K. Hashimoto, "Kidney Cancer Detection from CT Images by Transformer-Based Classifiers," *2023 14th IIAI International Congress on Advanced Applied Informatics (IIAI-AAI)*, Koriyama, Japan, 2023, pp. 456–461.
[21] S. R. Duggirala, S. Kollem, and R. L. Reddy, "An optimized SVM-based possibilistic fuzzy c-means clustering algorithm for tumor segmentation," *Multimedia Tools and Applications*, vol. 80, no. 1, pp. 409–437, 2021
[22] E. Yang, Y. Guan, B.-B. Koo, and J.-H. Kim, "3D Multi-Scale Residual Fully Convolutional Neural Network for Segmentation of Extremely Large-Sized Kidney Tumor," *Computer Methods and Programs in Biomedicine*, vol. 215, pp. 106616, 2022.
[23] G. Chen, C. Ding, Y. Li, X. Hu, X. Li, L. Ren, X. Ding, P. Tian, and W. Xue, "Prediction of Chronic Kidney Disease Using Adaptive Hybridized Deep Convolutional Neural Network on the Internet of Medical Things Platform," *IEEE Access*, vol. 8, pp. 100497–100508, 2020.
[24] A. Muhamed Ali, H. Zhuang, A. Ibrahim, O. Rehman, M. Huang, and A. Wu, "A machine learning approach for the classification of kidney cancer subtypes using miRNA genome data," *Applied Sciences*, vol. 8, no. 12, p. 2422, 2018.
[25] Y. Ren, H. Fei, X. Liang, D. Ji, and M. Cheng, "A hybrid neural network model for predicting kidney disease in hypertension patients based on electronic health records," *BMC Medical Informatics and Decision Making*, vol. 19, no. S2, Apr. 2019.
[26] G. Santini, N. Moreau, and M. Rubeaux, "Kidney tumor segmentation using an ensembling multi-stage deep learning approach. A contribution to the KiTS19 challenge," *arXiv preprint*, arXiv:1909.00735, 2019.
[27] G. Smith and R. Johnson, "Hybrid CNN for Kidney Disease Prediction," *IEEE IoT Journal*, vol. 6, no. 1, pp. 1001–1010, 2019.
[28] P. Kumar and R. N. Sharma, "Ensemble Learning for Kidney Disease Classification," *Journal of Computational Health Sciences*, vol. 10, no. 4, pp. 232–245, 2019.
[29] K. Rajkumar, S. Ashadapu, R. T. Sri Ramoju, C. Rajendra Prasad, T. Balelly, and Y. Srikanth, "Kidney Cancer Detection using Deep Learning Models," *2023 7th International Conference on Trends in Electronics and Informatics (ICOEI)*, pp. 979–984, 2023. DOI: 10.1109/ICOEI56765.2023.10125589.
[30] V. Gayathri, R. Gayathri, and K. Yogeshvaran, "Detection of Kidney Cancer Using Circularly Polarized Hexagonal Shape Microstrip Patch Antenna," *International Journal of All Research Education and Scientific Methods*, vol. 12, no. 3, pp. 3043–3048, 2024.
[31] M. S. Islam, K. P. Esselle, D. Bull, and P. M. Pilowsky, "Converting a Wireless Biotelemetry System to an Implantable System Through Antenna Redesign," *IEEE Transactions on Microwave Theory and Techniques*, vol. 62, no. 9, pp. 1890–1897, 2014.
[32] A. Kiourti, J. R. Costa, and C. A. Fernandes, "Miniature Implantable Antennas for Biomedical Telemetry: From Simulation to Realization," *IEEE Transactions on Biomedical Engineering*, vol. 59, no. 11, pp. 3140–3147, 2012.

[33] P. Soontornpipit, C. M. Furse, and Y. C. Chung, "Design of Implantable Microstrip Antenna for Communication With Medical Implants," *IEEE Transactions on Microwave Theory and Techniques*, vol. 52, no. 8, pp. 1944–1951, 2004.
[34] W. Lei, H. Chu, and Y. Guo, "Design of a Circularly Polarized Ground Radiation Antenna for Biomedical Applications," *IEEE Transactions on Antennas and Propagation*, vol. 64, no. 6, pp. 2535–2540, 2016.
[35] M. Zada and H. Yoo, "A Miniaturized Triple-Band Implantable Antenna System for Bio-Telemetry Applications," *IEEE Transactions on Antennas and Propagation*, vol. 66, no. 8, pp. 4301–4311, 2018.
[36] M. K. Magill, G. A. Conway, and W. G. Scanlon, "Tissue-Independent Implantable Antenna for In-Body Communications at 2.36–2.5 GHz," *IEEE Transactions on Antennas and Propagation*, vol. 65, no. 9, pp. 4406–4417, 2017.
[37] C. L. Yang, C. L. Tsai, and S. H. Chen, "Implantable High-Gain Dental Antennas for Minimally Invasive Biomedical Devices," *IEEE Transactions on Antennas and Propagation*, vol. 61, no. 5, pp. 2380–2387, 2013.
[38] C. Prathima, J. V. Rao, P. Sarath, P. Prathyusha, O. Karthik, and S. Aastha, "Data augmentation and hyperparameter tuning boost food image recognition," *2024 IEEE Int. Conf. Inf. Technol., Electron. Intell. Commun. Syst. (ICITEICS)*, pp. 1-5, 2024.
[39] M. Pathak, D. Chaudhary, K. Sharma, A. K. Sharma, A. Gupta, and B. K. Sharma, "A robust EfficientNet architecture for brain tumor classification and identification using MRI image," *2023 11th Int. Conf. Intell. Syst. Embedded Des. (ISED)*, Dehradun, India, 2023, pp. 1-5, doi: 10.1109/ISED59382.2023.10444597.
[40] M. Li, L. He, C. Lei, and Y. Gong, "Fine-grained image classification model based on improved SqueezeNet," *2021 IEEE 5th Adv. Inf. Technol., Electron. Autom. Control Conf. (IAEAC)*, Chongqing, China, 2021, pp. 393-399, doi: 10.1109/IAEAC50856.2021.9390687.
[41] M. Pavithra and B. T. Geetha, "Prediction of Chronic Kidney Cancer Using RBF Support Vector Machine Compared with Random Forest for Better Accuracy," *International Conference on Innovative Computing, Intelligent Communication and Smart Electrical Systems (ICSES)*, Chennai, India, 2022, pp. 1-5, doi: 10.1109/ICSES55317.2022.9914342.